A EUROPEAN JOURNAL

CHEMPHYSCHEM

OF CHEMICAL PHYSICS AND PHYSICAL CHEMISTRY

Accepted Article

Title: The Poynting's theorem-based thermogenic control of collective magnetic nanoparticles in the presence of alternating magnetic field

Authors: Jianfei Sun; Fengguo Fan; Peng Wang; Siyu Ma; Lina Song; Ning Gu

To be cited as: ChemPhysChem 10.1002/cphc.201600787

Link to VoR: http://dx.doi.org/10.1002/cphc.201600787

A Journal of

ChemPubSoc Europe

www.chemphyschem.org

WILEY-VCH

Orientation-dependent thermogenesis of assembled magnetic nanoparticles in the presence of alternating magnetic field

Jianfei Sun*[a], Fengguo Fan[a], [b], Peng Wang[a], Siyu Ma[a], Lina Song[a] and Ning Gu*[a]

Abstract: Thanks to the thermogenesis in the presence of alternating magnetic field, magnetic nanoparticles have exhibited a promising role in local heating *in vivo*. However, the flexible control of thermogenesis for the given nanomaterials remains challenging. Here, we proposed that the thermogenesis of assembled magnetic nanoparticles can be controlled by orientation of the film relative to external field. This idea arises from the principle of energy conservation that is formulated by the Poynting's theorem in electromagnetics. We firstly proved the thermogenesis of magnetic nanoparticles under alternating magnetic field was directly relative with the energy flux of field rather than the field intensity. Then alteration of orientation can lead to different incident electromagnetic energy for the film of nanoparticles, where cross-section of energy absorption played a crucial role. We developed a method to directly measure the complex susceptibility of assembled film to confirm this point. This work will be of great importance for the applications based on the electromagnetic energy conversion of nanomaterials.

Thanks to the thermogenesis in the presence of alternating magnetic field, magnetic nanoparticles have exhibited a promising role in local heating *in vivo*, which can be used for hyperthermal therapy[1], controlled release of drugs[1b, 2], deep brain stimulation[3] and so on. There have been numerous reports about the design of synthesis route to realize better magnetothermal performance,[4] among which one significant advance recently is the exchange-coupled magnetic nanoparticles with efficient heat induction.[5] As far as the magnetic nanoparticles are concerned collectively, it was also discovered that the interaction between nanoparticles can significantly influence the collective thermogenesis.[6] Although the thermogenic mechanism of one nanoparticle seems clear, how to control the collective thermogenesis flexibly for the given nanomaterials remains challenging. This issue will become more important with the emerging application of two-dimensional granular film-based devices because the collective thermogenesis of granular film is dependent upon not only the nanoparticles but also the interactions between them. With the architecture augmenting, the thermogenic control by composition of individual nanoparticles is increasingly difficult to apply in whole system. Here, we proposed that the thermogenesis of assembled film of magnetic nanoparticles can be controlled by altering the orientation of film relative to the external field. The mechanism lies in the different incident energy which is formulated by the Poynting's theorem in electromagnetics.[7] The magnetothermal effect can be regarded as a conversion from electromagnetic energy into thermal energy. Thus, the thermogenesis can be controlled by the input energy from alternating magnetic field. This strategy has the advantages of flexibility, simplicity and substantivity. In practical application, this means is a complement to the tailored synthesis of nanomaterials. Furthermore, the cross-section of energy absorption was found to play an important role in the orientation-dependent thermogenesis. We developed a method to measure the complex susceptibility of assembled film. With these data, the role of collective cross-section of energy absorption in the thermogenic regulation process was proved.

For a time-varied electromagnetic field, the energy is propagating along direction of the energy flux density vector, i. e. the Poynting's vector ($\vec{S}$, $\vec{S}=\vec{E}\times\vec{H}$) rather than that of the magnetic field intensity ($\vec{H}$). For a macroscopically continuous medium, the input energy (E_{in}) from the electromagnetic field into the medium relies on both the energy flux density and the projected area ($\vec{s}$) of the medium in the energy flux density vector, which can be expressed by the Poynting's theorem:

$$E_{in}=\iint_s \frac{1}{2}(\vec{E}\times\vec{H}^{*})\cdot d\vec{s}=E_m+E_e+E_j+E_{wattless} \quad (1)$$

where E_m, E_e, E_j and $E_{wattless}$ mean the magnetic loss, the electric loss, the joule heat and the wattless power, respectively. Because of the energy conservation, their sum should be equal to the input energy. Seen from Eq. 1, the incident energy can be tuned by the control of interaction between the medium and the Poynting's vector, including the morphology of medium and the relative orientation of medium with the field if the alternating magnetic field is given. As far as the aggregates of nanoparticles are concerned, the case is a bit different because the medium is not microscopically continuous. If there is negligible interaction between nanoparticles, the energy absorption should be sum of the individual nanoparticles. That means

$$E_{in}=\sum_{i=1}^{N}E_{in}^{i} \quad (2)$$

where E_{in} is the input energy of granular film, E_{in}^{i} the input energy of individual nanoparticle and N the number of nanoparticles. For one magnetic nanoparticle, the thermogenesis in unit time is expressed by

$$P=(\mu H\omega\tau)^{2}/[2\tau kTm(1+\omega^{2}\tau^{2})] \quad (3)$$

where μ is magnetic moment of nanoparticle, H and ω intensity and angle frequency of alternating magnetic, respectively, τ relaxation time of nanoparticle, m mass of nanoparticle and k and T Boltzmann's constant and ambient

[a] Dr. J. Sun, F. Fan, P. Wang, S. Ma, Dr. L. Song and Prof. Dr. N. Gu
State Key Laboratory of Bioelectronics, Jiangsu Key Laboratory of Biomaterials and Devices, School of Biological Science and Medical Engineering
Southeast University
Dingjiaqiao 87#, Nanjing, P. R. China
E-mail: sunzaghi@seu.edu.cn, guning@seu.edu.cn
[b] F. Fan
Department of Physics
Shangqiu Normal College
Pingyuan Road 55#, Shangqiu, Henan, P. R. China

temperature, respectively.[8] When the interaction between nanoparticles is incapable of neglect, the input energy on the whole granular film should add influence of the magnetic couplings on the basis of Eq. 1. That is

$$E_{in} = \sum_{i=1}^{N} E_{in}^{i} + \sum_{i<j}^{N} E_{in}^{ij} \quad (4)$$

where E_{in}^{ij} means the energy absorption resulting from the interaction between two magnetic nanoparticles. Regarding the magnetic couplings between nanoparticles as "virtual particles", the thermogenesis may have the similar form as Eq. 3, where the "μ" and "τ" positively depends upon the strength of interparticulate couplings. Seen from Eq. 4, the thermogenesis of aggregated magnetic nanoparticles can be tuned not only by the composition of individual nanoparticles but also by the interaction between nanoparticles. Furthermore, seen from Eq. 3, if the interaction between nanoparticles is adequately strong, the influence from the interaction between nanoparticles may overwhelm that from the nanoparticles themselves.

Here, the magnetothermal effect of two-dimensional assembled film of iron oxide nanoparticles was chosen as a model due to its role in theoretic analysis and practical application. For one thing, the two-dimensional morphology is succinct theoretically. In addition, the electromagnetic energy for iron oxide nanoparticles here is mainly consumed on the magnetic loss, excluding the influence from electric loss and joule heat. For another, the model is significant for application. Due to the flexibility and tailorability,[9] the assembled film of nanoparticles have been extensively used in the fabrication of flexible devices and surface coating of biomedical materials.[10] Thus, the investigation in two-dimensional film of magnetic nanoparticles will directly redound to guide the practical application of magnetothermal effect. For instance, we can properly design the structure of nanoparticles-based devices so that the energy can be utilized as much as possible. Moreover, the dependence of thermogenesis upon morphology can illume the intelligent control of biomedical devices, such as flexible film of magnetic nanoparticles. Finally, the energy viewpoint can account for the thermogenesis of hybridized nanomaterials. Introduction of matters with high electric or magnetic polarizability will also enhance the thermogenesis of alternating magnetic field.

In our experiments, the two-dimensional film of nanoparticles was fabricated by layer-by-layer (LBL) assembly of γ-Fe_2O_3 nanoparticles on a glass substrate of 25mm diameter (Fig. 1a). The LBL assembly can produce the contact, uniform and reproducible films of nanoparticles with controllable thickness.[11] As the control, one mold was made to contain the colloidal sample of γ-Fe_2O_3 nanoparticles whose diameter and thickness were 25mm and 1.5mm, respectively (Fig. 1b). The γ-Fe_2O_3 colloidal nanoparticles were synthesized with co-precipitation method and the physicochemical parameters were shown in Supporting Information, Fig. S1. It was seen that the colloid was polydispersed and negatively charged. The size was about 12nm. PDDA (Poly-acrylamide-co-diallyldimethylammonium chloride) was used as polymer partner to make the LBL assembly of γ-Fe_2O_3 nanoparticles. SEM images of fabricated films after 20-layer assembly were shown in Fig. 1c, d where the assembled film of nanoparticles seemed uniform, contact and homogeneous macroscopically but cluster-like microscopically. Here one point should be noticed that the nanoparticles were capped by a layer of PDDA molecules so that they were a bit separated rather than closely contacted (Fig. 1d inset).

The alternating magnetic field in our experiments was generated by a 4-turns coil which was schematically shown in Fig. 2a. The frequency and field intensity were fixed to about 390KHz and 12mT, respectively. Then the energy flux density ($\vec{S}$) was simulated in the absence and presence of the magnetic film, respectively (Fig. 2b). Corresponding distribution of magnetic field ($\vec{H}$) and induced electric field ($\vec{E}$) were also simulated, respectively (Supporting Information, Fig. S2). Seen from the simulation, the energy flux was radial in x-y plane while the magnetic field intensity was along z direction. The presence of magnetic film seemed to enhance the local energy flux if the film was parallel to $\vec{H}$. This case hinted us that the thermogenesis of magnetic nanoparticles in the presence of alternating magnetic field should be dependent upon orientation of the sample. However, the influence of sample placement was seldom considered experimentally. This may be actually inessential for the magnetic nanoparticles in colloidal suspension. The thermogenic measurement of γ-Fe_2O_3 colloidal suspension in our lamella-like mold proved this point. The mold was put in different orientations relative to $\vec{H}$ (from 0° to 90°) and the results were nearly of total overlap (Fig. 2c). Based on Eq.1, the energy of electromagnetic field acting on medium relies upon the projected area in the Poynting's vector. Therefore, the thermogenesis of γ-Fe_2O_3 colloidal suspension seemed independent upon the input energy of alternating magnetic field. However, when the LBL-assembled films of nanoparticles were put into alternating magnetic field, the thermogenic curves increasingly exhibited dependence upon the orientation with the thickness growing (Fig. 2d-f). For the assembled film of 3 layers, the thermogenic curves were similar to that of colloidal suspension. When the layer number arrived at 20 or more, an evident correlation between the equilibrium temperature and the inclined angle of film emerged. Here the linear correlative coefficient can exceed 0.9. Interestingly, it was along the direction parallel to $\vec{H}$ that the LBL-assembled film yielded the maximal heating temperature. This seemed opposite to our intuition because the interacted area between the film and $\vec{H}$ was minimal in this direction. Therefore, the thermogenesis of magnetic nanoparticles is possibly dominated by other factors rather than the field intensity.

Due to its radial distribution, the Poynting's vector was considered to account for this phenomenon. In the direction along $\vec{H}$, the interacted area between the Poynting's vector and the film of nanoparticles is maximal. Based on Eq. 1, the film of nanoparticles can get maximal energy from the alternating magnetic field. Therefrom, it was hypothesized that the orientation-dependent thermogenesis actually rooted in the Poynting's theorem. To confirm this point, three LBL-assembled films were fabricated. They had same surface areas but different projected areas in the Poynting's vector. The morphological photos of these samples were shown in Fig. 3a. In our experiments, the top and bottom facets of these samples were shielded from the contact with colloid suspension and their lateral areas were intentionally designed to be identical. Thus,

the ratio of projected areas for cylinder, square column and triangle column on the Poynting's vector was 1.66:1.3:1 (Fig. 3b). Based on Eq. 1, the ratio of heating temperatures should be positively proportional to the ratio of projected areas. The magnetothermogenic measurements proved this point (Fig. 3c), where the linear correlative coefficient between the ratio of the projected areas and that of the heating temperatures was calculated to reach 0.997 (Fig. 3d). Thus, for the closely assembled nanoparticles, the magnetothermogenic effect can be regulated by the projected area of collective nanoparticles in the Poynting's vector.

Then based on Eq. 3 and Eq. 4, the thermogenesis for assembled film of nanoparticles can be further enhanced by regulating the interaction between nanoparticles. This also means there is more energy converted into the heat rather than the wattless power. Because the wavelength of alternating magnetic field in our experiments was about 750m, either the colloidal suspension or the assembled film can be penetrated by the electromagnetic wave facilely. Thus, the energy absorption by the nanomaterials became a critical issue. Here, the energy absorption of medium can be indicated by the so-called energy absorption cross-section which obeys the following formula:

$$\sigma = 4\pi\omega V(\alpha_e'' + \alpha_m'')/c \quad (5)$$

where σ is the cross-sections of absorption, ω the angle frequency of alternating magnetic field, V the volume of particle, c the velocity of light in vacuum, α_e'' and α_m'' the imaginary parts of electric and magnetic polarizability of the particle, respectively.[12] As far as the homogeneous film of γ-Fe_2O_3 nanoparticles was concerned, the magnetic polarizability was degraded to the susceptibility. The colloidal suspension and the assembled film of γ-Fe_2O_3 nanoparticles can be regarded as the macroscopically continuous media. Then the Poynting's theorem was applied to them. The input energy was denoted as $E_{//}$ and $E_{\perp}$, meaning that the Poynting's vector was parallel to the medium and perpendicular to the medium, respectively. Certainly, $E_{//} << E_{\perp}$. For the colloidal suspension of 0.089mg ml^{-1} (concentration in our experiment), the effective susceptibility was actually very small because the magnetic nanoparticles just occupied a tiny portion of the suspension. According to Eq. 5, the absorption cross-section was also very small. This meant the energy absorption for colloidal suspension was so weak that even the minimal input energy was enough for the demand of nanoparticles to heat up. For this reason, the thermogenesis of γ-Fe_2O_3 colloidal suspension showed little difference with the alteration of input energy. The superfluous energy was actually dissipated as the wattless power. This mechanism was also applicable for the film of nanoparticles with small assembled layer number. Here, the density of nanoparticles on substrate was very low. However, for the closely-assembled nanoparticles, there were strong magnetic couplings between nanoparticles.[13] The magnetic coupling can greatly augment the collective susceptibility of assembled nanoparticles like magnetic bonding.[14] Our previous reports also partly proved this point that the assembly of magnetic nanoparticles can lead to the transition of collective magnetic property from superparamagnetism into weak ferromagnetism owing to the dipolar coupling of magnetic moments.[15] Magnetization simulation for a chain of magnetic particles also showed that there were magnetic responses in the spaces between particles which can be regarded as the magnetic "virtual particles" (Supporting Information, Fig. S3a). Seen from the simulation of magnetothermogenesis, there was also thermogenesis in the spaces between particles (Supporting Information, Fig. S3b). This meant the assembled particles need more electromagnetic energy to heat up, just as manifested by Eq. 4. As a result, the thermogenesis of assembled film was changed along with the different incident energy flux of alternating magnetic field. This concept was schematically shown in Fig. 4.

Based on Eq. 5, the energy absorption cross-section is directly relative with the imaginary part of complex permeability. Thus, we developed a method to measure the complex permeability of assembled film under the frequency of experimental alternating magnetic field. For the assembled films of 3 layers, 10 layers and 20 layers, respectively, the measured results of complex permeability were shown in Supporting Information, Fig. S4. It was seen that the value of μ'' (imaginary part of permeability) was truly augmented with adding number of assembled layers. Thus, the energy absorption cross-section was also enlarged, which was in accordance with the experimental results of thermogenic measurement. Then, it was further inferred that the magnetic nanoparticles can have the more thermogenesis collectively if the imaginary part of collective complex permeability was increased. Based on this idea, we fabricated three assembled films of γ-Fe_2O_3 nanoparticles with nearly identical microstructure but different magnetic couplings between nanoparticles. The films were fabricated by the static magnetic field-directed assembly, the alternating magnetic field-directed assembly and the natural drying of nanoparticles, respectively. The morphological images and the simulated arrangements of magnetic moments for these samples were shown in Fig. 5a-c. They were seen to have little difference in morphology while the arrangements of magnetic moments were significantly different. The arrangement of magnetic moments for magnetostatic field-directed assembly was head-to-tail while that for alternating magnetic field-directed assembly was vortex-like. Different from both, the magnetic moments were disordered for the naturally-dried sample. The heating curves of three samples were shown in Fig. 5d, where the magnetostatic field-assembled sample exhibited the maximal heating temperature and the naturally-dried sample had the minimal heating temperature. VSM (Vibrating Sample Magnetometer) and FMR (FerroMagnetic Resonance) had been used to characterize the magnetic property of the three samples (Supporting Information, Fig. S5). The results showed that the magnetic coupling for the magnetostatic field-directed sample was slightly stronger than that of the alternating magnetic field-directed sample or that of the naturally-dried sample. However, the latter two samples seemed little different. The measured results of μ'' with our method were shown in Fig. 5e (The results of $|\mu|$ and μ' were shown in Supporting Information, Fig. S6.). Seen from the results, the magnetostatic field-directed assembly led to the maximal value of imaginary part of complex permeability while the natural drying caused the minimal value. Moreover, the values for magnetostatic field-directed sample and alternating magnetic field-directed sample were approximating but both were significantly greater than that for naturally-dried sample. Based on Eq. 5, although the physical

areas of three films were identical, their energy absorption cross-sections were different. Thus, the magnetic coupling between particles can enhance the collective thermogenesis of magnetic nanoparticles.

In conclusion, it was proposed that the thermogenesis of magnetic nanoparticles in the presence of alternating magnetic field is more dependent upon the energy flux density rather than the field intensity. The thermogenesis can be regulated based on the Poynting's theorem. The critical issue lied in the cross-section of energy absorption which was highly correlative with the interaction between nanoparticles. Due to the fundamental importance of the Poyting's theorem in electromagnetics, this work will deepen the understanding of thermogenic mechanism of magnetic nanomaterials and enrich the application of magnetothermal effect.

Experimental Section

LBL Assembly The colloidal suspension of γ-Fe_2O_3 nanoparticles was concentrated to 2mg/ml for the layer-by-layer assembly. The PDDA (poly-diallydimethylammonium chloride) solution was diluted to 2% with ultra-pure water. A glass slide was firstly treated by the boiling mixture of H_2SO_4 and H_2O_2 (volume ratio: 7:3) for 2h. After that, the glass slide was washed by the ultra-pure water repeatedly and finally dried by N_2 gas stream. Then, the glass slide was put into the PDDA solution and the colloidal suspension of γ-Fe_2O_3 nanoparticles for 10min and 20min, respectively. The γ-Fe_2O_3 nanoparticles were adsorbed on the glass slide due to the electrostatic interaction which brought about the formation of one bilayer. When the soak in one solution terminated, the glass slide was washed by ultra-pure water repeatedly and finally dried by N_2 gas stream. The steps were duplicated leading to the layer-by-layer assembly of nanoparticles.

The simulation of alternating magnetic field and thermogenesis of particles The Poynting's vector simulation of alternating magnetic field was executed with Ansoft software and the magnetothermogenesis of particles was done with Comsol software. Both methods are based on finite element analysis. In the Ansoft simulation, the inner diameter of coil was 45mm. The height was 20mm and the number of windings was 4. The excitation current was 15A and the frequency was 390KHz. The diameter of film was 20mm and the thickness was 2mm. In the Comsol simulation, the diameter of particle was 1mm. The space was 0.2mm. The field intensity was 34KA/m and the frequency was 390KHz.

The measurement of magnetothermal heating The measurement of magnetothermogenesis of samples was by an optical-fibre temperature sensor (FISO UMI 8, Canada, measuring range: -4°C-100°C). The sample was fixed on a holder with different inclined planes so that the inclined angles of sample can be changed. Then the holder with sample was put into an alternating magnetic field (390KHz, 12mT) and the optical fibre was stuck to the surface of film to collect the signal. The data of heating temperature versus time were recorded with the Universal Multichannel Instrument (Canada) and transferred to a computer for analysis in real time.

The measurement of complex permeability The measurement of complex permeability for film-like sample was based on the data of surface impedance which was obtained from an impedance analyser (Agilent 4294A, the United States, measuring range: 40Hz-110MHz). The film was connected with the adapter of impedance analyzer by a pair of alligator clips. Then after calibration, the machine can measure the impedance along the surface of film. The original data were the module and phase angle of impedance, which were denoted as $|\zeta|$ ($\zeta=\zeta^{'}+j\zeta^{''}$) and θ. Based on the definition of surface impedance, $\zeta=\sqrt{\frac{\mu}{\varepsilon}}$, where μ ($\mu=\mu^{'}+j\mu^{''}$) is the complex permeability and ε ($\varepsilon=\varepsilon^{'}+j\varepsilon^{''}$)is the permittivity. Because the macroscopic iron oxide is semiconductor, it was supposed that the aggregation of γ-Fe_2O_3 nanoparticles will have little influence on ε. Thus, if the ε is known, the μ can be calculated from the data of impedance. Here, the collective ε of assembled γ-Fe_2O_3 nanoparticles was replaced by that of assembled α-Fe_2O_3 nanoparticles which is identical with γ-Fe_2O_3 in composition but slightly different in crystalline structure. Due to the paramagnetism, the μ of assembled α-Fe_2O_3 nanoparticles can be considered as 1. Then the ε of assembled α-Fe_2O_3 nanoparticles can be calculated from the impedance data of α-Fe_2O_3 film. Thus, the μ of assembled film of γ-Fe_2O_3 nanoparticles can be calculated with the same calculation process. As for the calculation, the measured data of ζ and θ were firstly fitted as a function, respectively. Then we made derivation to on frequency so that the μ can be obtained by solving the differential equation of impedance versus frequency. The impedance data of assembled film of α-Fe_2O_3 nanoparticles showed that the ε truly kept constant in the range of experimental frequency.

Acknowledgements

This work was supported by the National Basic Research Program of China (2013CB733801) and the National Science Foundation of China (21273002). Jian F. Sun is also thankful to the supports from the special fund for the top doctoral thesis of Chinese Education Ministry (201174). Jian F. Sun and Ning Gu are thankful to the supports from Collaborative Innovation Center of Suzhou Nano Science and Technology.

Keywords: magnetothermal effect • magnetic nanoparticles • energy absorption • bioelectronics • LBL assembly

[1] a) M. Bañobre-López, A. Teijeiro, J. Rivas, *Rep. Pract. Oncol. Radiother.* **2013**, *18*, 397–400. b) L. H. Reddy, J. L. Arias, J. Nicolas, P. Couvreur, *Chem. Rev.* **2012**, *112*, 5818-5878.

[2] S. Mura, J. Nicolas, P. Couvreur, *Nat. Mater.* **2013**, *12*, 991-1003.

[3] a) R. Chen, G. Romero, M. G. Christiansen, A. Mohr, P. Anikeeva, *Science* **2015**, *347*, 1477-1480. b) S. A. Stanley, L. Kelly, K. N. Latcha, S. F. Schmidt, X. Yu, A. R. Nectow, J. Sauer, J. P. Dyke, J. S. Dordick, J. M. Friedman, *Nature* **2016**, 531, 647-650.

[4] a) A. Meffre, B. Mehdaoui, V. Kelsen, F. Pier Fazzini, J. Carrey, S. Lachaize, M. Respaud, B. Chaudret, *Nano Lett.* **2012**, *12*, 4722-4728. b) Y. V. Kolen'ko, M. Bañobre-López, C. Rodríguez-Abreu, E. Carbó-Argibay, A. Sailsman, Y. Piñeiro-Redondo, M. F. Cerqueira, D. Y. Petrovykh, K. Kovnir, I. Oleg Lebedev, J. Rivas, *J. Phys. Chem. C* **2014**, *118*, 8691-8701. c) M. L. Etheridge, J. C. Bischof, *Annal. Biomed. Eng.* **2013**, *41*, 78-88.

[5] J.-H. Lee, J.-T. Jang, J.-S. Choi, S. H. Moon, S.-H. Noh, J.-W. Kim, J.-G. Kim, I.-S. Kim, K. I. Park, J. Cheon, *Nat. Nanotechnol.* **2011**, *6*, 418-422.

[6] a) D. Serantes, K. Simeonidis, M. Angelakeris, O. Chubykalo-Fesenko, M. Marciello, M. del P. Morales, D. Baldomir, C. Martinez-Boubeta, *J. Phys. Chem. C* **2014**, *118*, 5927-5934. b) C. Haase, U. Nowak, *Phys. Rev. B* **2012**, *85*, 45435-45439. c) L. C. Branquinho, M. S. Carrião, A. S. Costa, N. Zufelato, M. H. Sousa, R. Miotto, R. Ivkov, A. F. Bakuzis, *Sci. Rep.*

2013, *3*, 2887-2896. D. Ling, N. Lee, T. Hyeon, *Acc. Chem. Res.* **2015**, *48*, 1276-1285.

[7] I. Campos, J. L. Jimenez, *Eur. J. Phys.* **1992**, *13*, 117-121.

[8] M. Ma, Y. Wu, J. Zhou, Y. K. Sun, Y. Zhang, N. Gu, *J. Mag. Mag. Mater.* **2004**, *268*, 33-39.

[9] a) Y. Chen, Z. Ouyang, M. Gu, W. Cheng, *Adv. Mater.* **2013**, *25*, 80-85. b) P. S. Cendula, Kiravittaya, I. Mönch, J. Schumann, O. G. Schmidt, *Nano Lett.* **2011**, *11*, 236-240. c) K. J. Si, D. Sikdar, Y. Chen, F. Eftekhari, Z. Xu, Y. Tang, W. Xiong, P. Guo, S. Zhang, Y. Lu, Q. Bao, W. Zhu, M. Premaratne, W. Cheng, *ACS Nano* **2014**, *8*, 11086-11093.

[10] a) M. Segev-Bar, H. Haick, *ACS Nano* **2013**, *7*, 8366-8378. b) D. Campoccia, L. Montanaro, C. R. Arciola, *Biomaterials* **2013**, *34*, 8533–8554.

[11] L. Xu, W. Ma, L. Wang, C. Xu, H. Kuang, N. A. Kotov, *Chem. Soc. Rev.* **2013**, *42*, 3114-3126.

[12] L. D. Landau, E. M. Lifshitz, L. P. Pitaevskii, *Electrodynamics of Continuous Media*, Elsevier, Singapore, **2007**.

[13] B. Su, W. Guo, L. Jiang, *Small* **2015**, *11*, 1072-1096.

[14] S. Ghosh, I. K. Puri, *Faraday Discuss.* **2015**, *181*, 423-435.

[15] a) J. F. Sun, X. Liu, J. Q. Huang, L. N. Song, Z. H. Chen, H. Y. Liu, Y. Li, Y. Zhang, N. Gu, *Sci. Rep.* **2014**, *4*, 5125-5133. b) K. Hu, J. F. Sun, Z. B. Guo, P. Wang, Q. Chen, M. Ma, N. Gu, *Adv. Mater.* **2015**, *27*, 2507-2514.

Figure 1: characterization of the experimental samples. a) photo of the LBL-assembled film of γ-Fe_2O_3 nanoparticles (Φ=25mm). b) photos (top view and side view) of the mould containing colloidal suspension of γ-Fe_2O_3 nanoparticles (Φ=25mm). c) SEM image of the LBL-assembled film of γ-Fe_2O_3 nanoparticles with low magnification. d) SEM image of the LBL-assembled film of γ-Fe_2O_3 nanoparticles with high magnification. Inset, SEM image of sparse nanoparticles capped by a layer of PDDA molecules.

Figure 2: Thermogenic measurement of magnetic nanoparticles. a) schematic carton of thermogenic measurement for the film-like samples in the experimental alternating magnetic field. The inclined angle θ is indicated by the angle between the magnetic field and diameter of film. b) simulations of the Poynting's vector for the alternating magnetic field in the absence and presence of the film, respectively. It seemed that the energy flux was enhanced when the film was parallel to the field intensity. c) thermogenic curves of γ-Fe_2O_3 colloidal suspension with different inclined angle in the presence of alternating magnetic field. d-f) thermogenic curves of γ-Fe_2O_3 assembled film with different inclined angle in the presence of alternating magnetic field. The number of assembled layers of d), e) and f) was 3, 10 and 20, respectively.

Figure 3: Validation of relationship between the thermogenesis and the projected area on the Poynting's vector. a) the photo of moulds with three shapes. The film of γ-Fe_2O_3 nanoparticles was assembled on them with LBL method. b) the schematic show of projected area on the Poynting's vector for the lateral area of different assembled films. Actually, the projection is the inscribed circle of different shapes. c) the thermogenic curves of different assembled films in the presence of alternating magnetic field. d) the linear correlation between the ratio of heating temperature and the ratio of projected area on the Poynting's vector. The values of triangular column were used as the benchmark, which meant the heating temperature and the projected area were regarded as 1 for the triangular column.

Figure 4: The conceptual scheme of the thermogenic mechanism for γ-Fe_2O_3 colloidal suspension and assembled films in the presence of alternating magnetic field. a) γ-Fe_2O_3 colloidal suspension under the alternating magnetic field of lateral incidence. b) γ-Fe_2O_3 colloidal suspension under the alternating magnetic field of frontal incidence. c) assembled film of γ-Fe_2O_3 nanoparticles under the alternating magnetic field of lateral incidence. d) assembled film of γ-Fe_2O_3 nanoparticles under the alternating magnetic field of frontal incidence. Although the alternating magnetic field is identical in these cases, the incident energy is dissimilar due to the different interacted area between energy flux and medium. However, the influence of incident energy is dependent upon the energy absorption cross-section. For γ-Fe_2O_3 nanoparticles in colloidal suspension, the energy absorption cross-section is too small to have significant response to the different incident energy. For assembled film of γ-Fe_2O_3 nanoparticles, the energy absorption cross-section is greatly augmented so that the thermogenesis is significantly dependent upon the incident energy.

Figure 5: Augmentation of energy absorption cross-section by magnetic coupling to enhance the thermogenesis of assembled film. a-c) the SEM images and the corresponding micro-magnetic simulation of assembled film of γ-Fe_2O_3 nanoparticles by magnetostatic field-directed assembly, alternating magnetic field-directed assembly and natural drying, respectively. d) the thermogenic curves for the assembled films of a-c). e) the calculated imaginary parts of assembled films of a-c with the surface-impedance method. Our method showed the complex permeability of samples by magnetostatic field-directed assembly and alternating magnetic field-directed assembly were obviously greater than that by natural drying but the former two samples just had small difference.

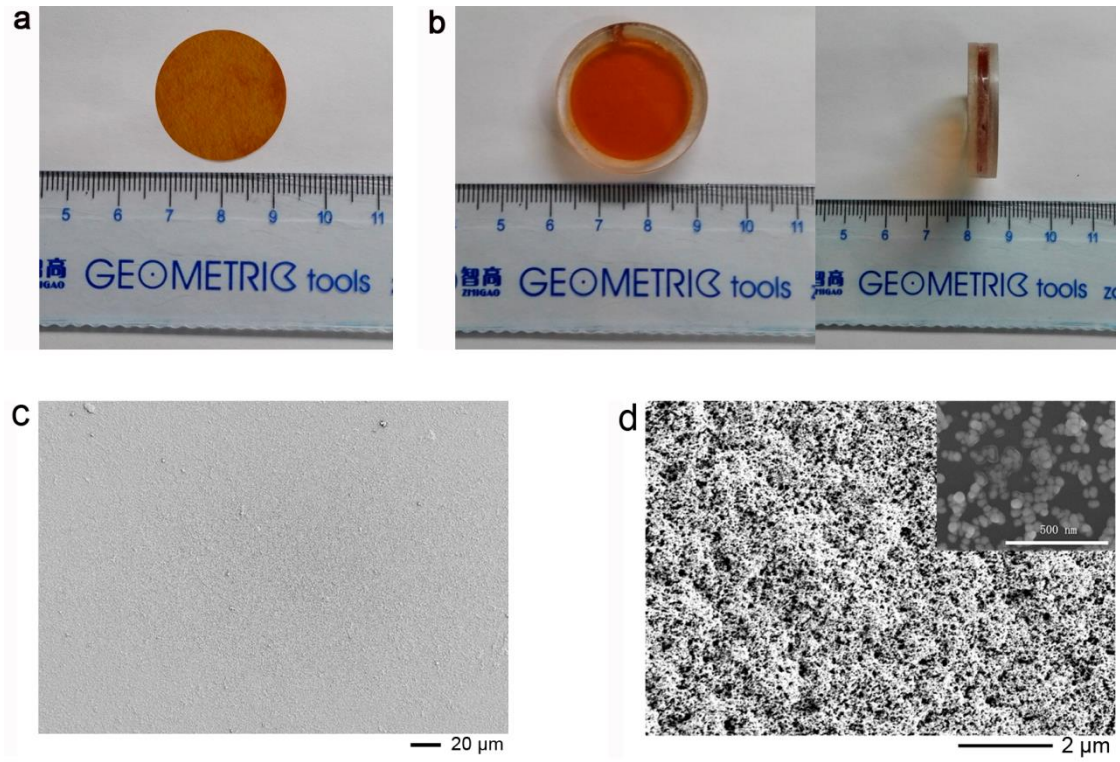

Figure 1: characterization of the experimental samples. a) photo of the LBL-assembled film of γ-Fe_2O_3 nanoparticles (Φ=25mm). b) photos (top view and side view) of the mould containing colloidal suspension of γ-Fe_2O_3 nanoparticles (Φ=25mm). c) SEM image of the LBL-assembled film of γ-Fe_2O_3 nanoparticles with low magnification. d) SEM image of the LBL-assembled film of γ-Fe_2O_3 nanoparticles with high magnification. Inset, SEM image of sparse nanoparticles capped by a layer of PDDA molecules.

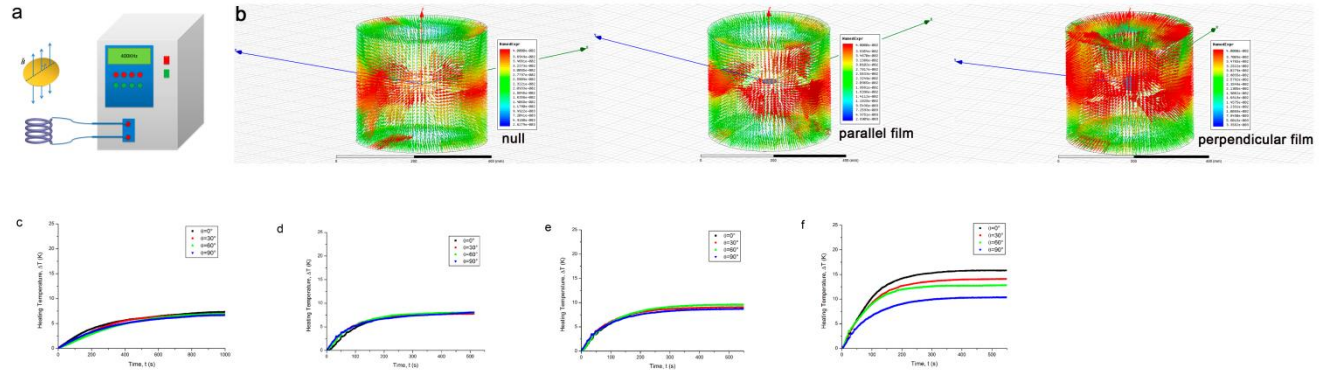

Figure 2: Thermogenic measurement of magnetic nanoparticles. a) schematic carton of thermogenic measurement for the film-like samples in the experimental alternating magnetic field. The inclined angle θ is indicated by the angle between the magnetic field and diameter of film. b) simulations of the Poynting's vector for the alternating magnetic field in the absence and presence of the film, respectively. It seemed that the energy flux was enhanced when the film was parallel to the field intensity. c) thermogenic curves of γ-Fe_2O_3 colloidal suspension with different inclined angle in the presence of alternating magnetic field. d-f) thermogenic curves of γ-Fe_2O_3 assembled film with different inclined angle in the presence of alternating magnetic field. The number of assembled layers of d), e) and f) was 3, 10 and 20, respectively.

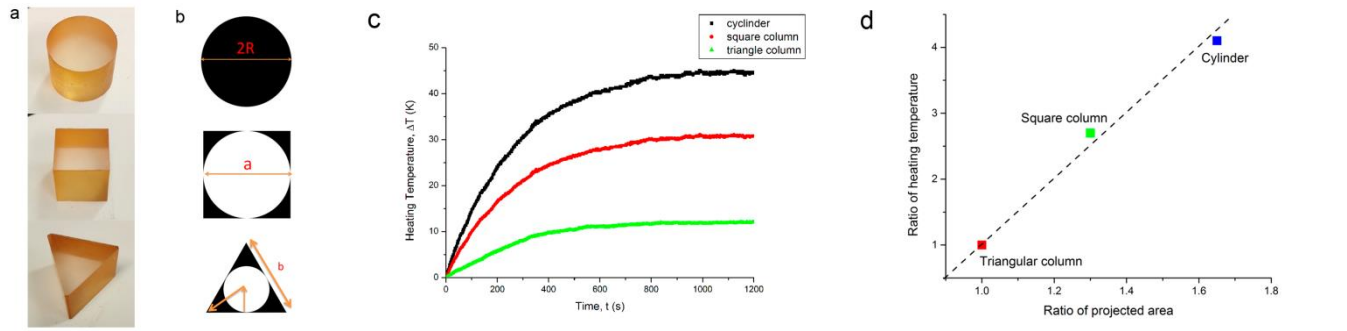

Figure 3: Validation of relationship between the thermogenesis and the projected area on the Poynting's vector. a) the photo of moulds with three shapes. The film of γ-Fe_2O_3 nanoparticles was assembled on them with LBL method. b) the schematic show of projected area on the Poynting's vector for the lateral area of different assembled films. Actually, the projection is the inscribed circle of different shapes. c) the thermogenic curves of different assembled films in the presence of alternating magnetic field. d) the linear correlation between the ratio of heating temperature and the ratio of projected area on the Poynting's vector. The values of triangular column were used as the benchmark, which meant the heating temperature and the projected area were regarded as 1 for the triangular column.

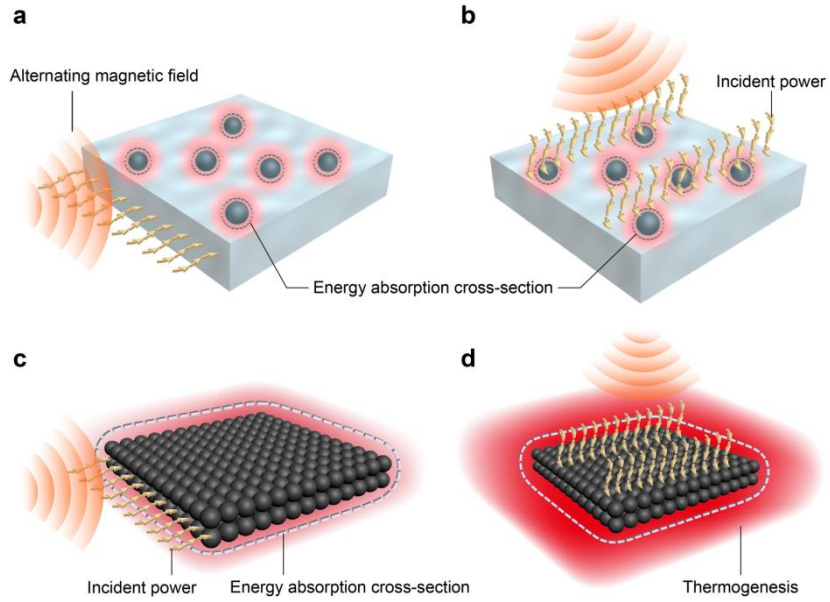

Figure 4: The conceptual scheme of the thermogenic mechanism for γ-Fe_2O_3 colloidal suspension and assembled films in the presence of alternating magnetic field. a) γ-Fe_2O_3 colloidal suspension under the alternating magnetic field of lateral incidence. b) γ-Fe_2O_3 colloidal suspension under the alternating magnetic field of frontal incidence. c) assembled film of γ-Fe_2O_3 nanoparticles under the alternating magnetic field of lateral incidence. d) assembled film of γ-Fe_2O_3 nanoparticles under the alternating magnetic field of frontal incidence. Although the alternating magnetic field is identical in these cases, the incident energy is dissimilar due to the different interacted area between energy flux and medium. However, the influence of incident energy is dependent upon the energy absorption cross-section. For γ-Fe_2O_3 nanoparticles in colloidal suspension, the energy absorption cross-section is too small to have significant response to the different incident energy. For assembled film of γ-Fe_2O_3 nanoparticles, the energy absorption cross-section is greatly augmented so that the thermogenesis is significantly dependent upon the incident energy.

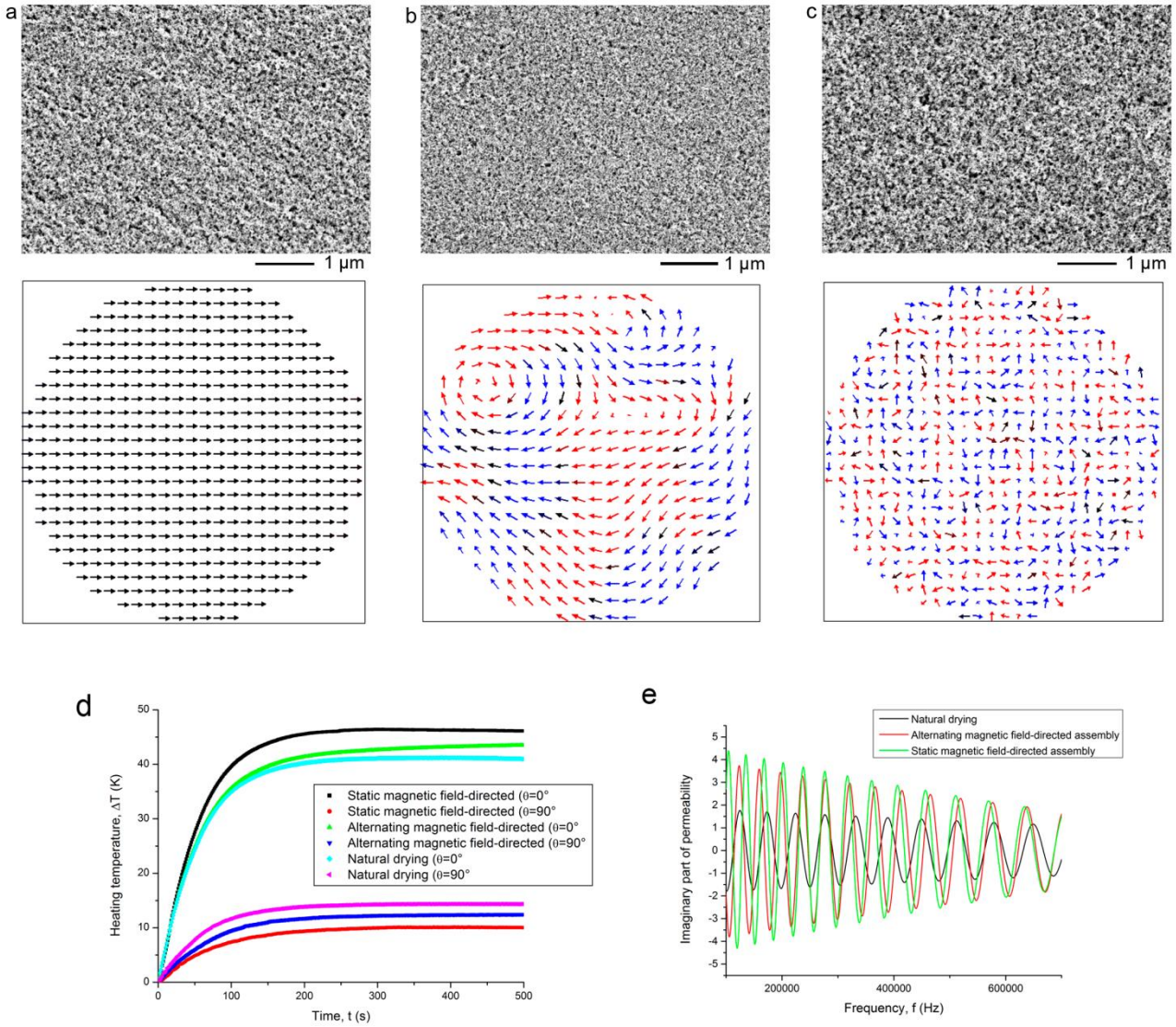

Figure 5: Augmentation of energy absorption cross-section by magnetic coupling to enhance the thermogenesis of assembled film. a-c) the SEM images and the corresponding micro-magnetic simulation of assembled film of γ-Fe_2O_3 nanoparticles by magnetostatic field-directed assembly, alternating magnetic field-directed assembly and natural drying, respectively. d) the thermogenic curves for the assembled films of a-c). e) the calculated imaginary parts of assembled films of a-c with the surface-impedance method. Our method showed the complex permeability of samples by magnetostatic field-directed assembly and alternating magnetic field-directed assembly were obviously greater than that by natural drying but the former two samples just had small difference.

Entry for the Table of Contents (Please choose one layout)

Layout 1:

COMMUNICATION

Text for Table of Contents

((Insert TOC Graphic here))

*Author(s), Corresponding Author(s)**

Page No. – Page No.

Title

Layout 2:

COMMUNICATION

((Insert 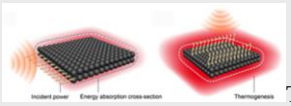 TOC Graphic here))

Assembled film of mangetic nanoparticles was fabricated with Layer-by-layer method as a model to explore the orientation-dependent thermogenesis in the presence of alternating magnetic field. It was found the thermogenesis can be regulated by altering the orientation of film relative to field, which mechanism lied in the different incident energy resulting from the interacting area between the film and the energy flux of field.

Jianfei Sun, Fengguo Fan, Peng Wang, Siyu Ma, Lina Song and Ning Gu**

Page No. – Page No.

Orientation-dependent thermogenesis of assembled magnetic nanoparticles in the presence of alternating magnetic field